THE ASTROPHYSICAL JOURNAL, 553:832–836, 2001 June 1

EARLY *CHANDRA* X-RAY OBSERVATIONS OF η CARINAE

F. D. SEWARD, Y. M. BUTT, M. KAROVSKA, A. PRESTWICH, AND E. M. SCHLEGEL
Smithsonian Astrophysical Observatory, 60 Garden Street, Cambridge, MA 02138

AND

M. CORCORAN
Laboratory for High Energy Astrophysics, NASA Goddard Space Flight Center, Greenbelt, MD 20771
Received 2000 September 25; accepted 2001 January 23

ABSTRACT

Subarcsecond-resolution *Chandra* observations of η Carinae reveal a $40'' \times 70''$ ring or partial shell of X-ray emission surrounding an unresolved bright central source. The spectrum of the central source is strongly absorbed and can be fitted with a high-temperature thermal continuum and emission lines. The surrounding shell is well outside the optical/infrared bipolar nebula and is coincident with the outer shell of η Car. The X-ray spectrum of the shell is much softer than that of the central source. The X-ray shell is irregular and only correlates well with optical features in which a bright X-ray knot coincides with a bright feature of the outer shell. Implications for the binary model of the central source are discussed.

Subject headings: stars: early-type — stars: individual (η Carinae) — X-rays: stars

1. INTRODUCTION

η Carinae has long been an object of mystery and a unique optical variable (see review by Davidson & Humphreys 1997). Initially of 4th to 2nd magnitude, it brightened to 1st magnitude in the 1830s and reached a maximum brightness of -1 in 1843. Between 1857 and 1869 it declined steadily from 1st to 7th magnitude. It underwent a second outburst in 1890 (Humphreys, Davidson, & Smith 1999), declined to and remained at 8th magnitude until about 1940, and has since brightened to almost 5th magnitude (Davidson et al. 1999). The central source of η Car has long been obscured by a small optical nebula, the homunculus, which *Hubble Space Telescope* (*HST*) observations have revealed to be a striking bipolar nebula (Hester et al. 1991; Humphreys & Davidson 1994). Measured expansion of the lobes indicate an origin at the time of the "Great Eruption" of 1843 (Walborn, Blanco, & Thackeray 1978). There is also a rapidly expanding disk in the plane between the bipolar lobes which seems to have originated during the later eruption in about 1890 (Smith & Gehrz 1998). A faint outer shell, with knots of fast-moving material, surrounds the bipolar structure (Walborn 1976).

η Car is now the brightest extrasolar infrared source, at wavelength 20 μm. We will use a distance of 2.3 kpc in this paper (Davidson & Humphreys 1997), but note that most of the previous X-ray work assumed a slightly larger distance of 2.6 kpc. An IR luminosity of $5 \times 10^6\ L_\odot$ was derived by Westphal & Neugebauer (1969), which is only a factor of ≈ 4 less than the optical luminosity during the Great Eruption (Davidson & Humphreys 1997). It is now believed that the source of energy is a massive object (or objects) at the center and that surrounding dust then reradiates the energy in the IR. Indeed, IR emission is observed to come from the bipolar nebula and the equatorial disk (Smith, Gehrz, & Krautter 1998). The central source, however, remains obscure at optical and IR wavelengths.

Since X-rays can penetrate dust, the X-ray band holds the promise of revealing more of the central object than ever. The first convincing observation was with *Einstein* (Chlebowski et al. 1984). This observation showed emission from an unresolved source in the vicinity of the central object and from an irregular outer region. This structure was confirmed with *ROSAT* observations by Corcoran et al. (1995), who discovered that the central source was variable. The *Einstein* spectrum was interpreted as the sum of a hard, strongly absorbed component and a soft component. A later observation with *ASCA* (Corcoran et al. 1998) showed the same dual nature, and with the better *ASCA* energy resolution, emission lines from Mg, Si, S, and Fe were detected in the spectrum. Neither the *Einstein* IPC nor the *ASCA* SIS instruments could spatially resolve the central source from the surrounding shell. A campaign to monitor high-energy X-rays with *RXTE* has been in progress since 1996 April. The variability observed is remarkable, showing a possible 85 day periodicity and a 3 month X-ray minimum (Ishibashi et al. 1999). These results have been interpreted with a model invoking colliding stellar winds and a massive binary system (Corcoran et al. 2000).

2. *CHANDRA* OBSERVATIONS

η Car was one of the first science observations done with *Chandra* (Weisskopf, O'Dell, & Van Speybroeck 1996). To demonstrate the capability of the observatory, η Car was observed on 1999 September 7 with the *Chandra* ACIS-I detector, first in timed exposure (TE) mode for 10,800 s then in continuous clocking (CC) mode for 12,200 s. During this period (and unbeknownst at the time) the energy resolution of the detector was degrading significantly as a result of radiation damage. Although the energy resolution of these spectra is considerably better than the present capability of the instrument, the calibration for this period of rapidly changing characteristics is poor.

The TE mode image is shown in Figure 1. A partial ring or shell of soft emission with dimensions $\sim 40'' \times 70''$ surrounds a bright central source. It is open in the south and lies closer to the central source in the west than in the east. There are two bright knots. Emission from the ring is soft, whereas the spectrum of the central source is hard and strongly absorbed. At energies below 1.0 keV, only the ring is seen.

The geometry and weakness of interior diffuse emission indicate a geometry more ringlike than shell-like. The orientation of this material, however, does not have a sensible

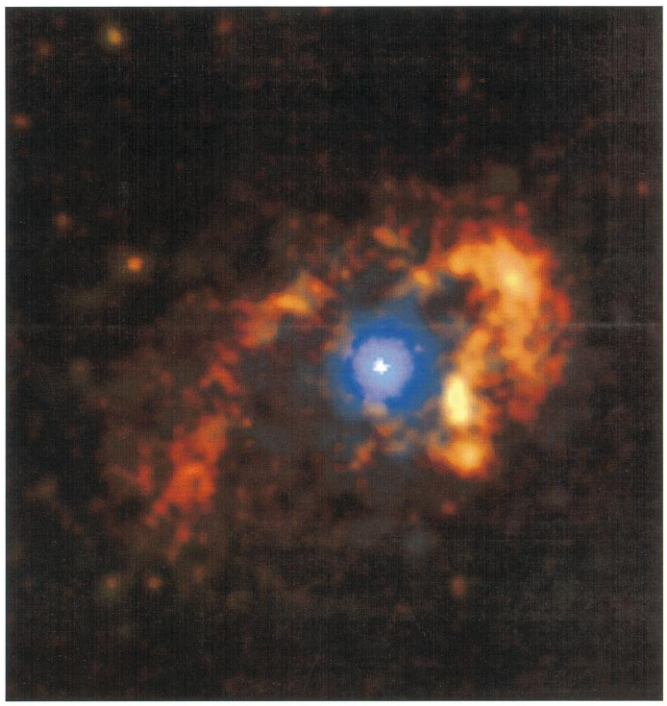

FIG. 1.—X-ray picture of η Car in the range 0.1–10 keV. A bright, strongly absorbed central source is surrounded by a partial ring of soft emission. Outer dimensions of the ring are $40'' \times 70''$. Data have been processed by an adaptive smoothing algorithm. Red indicates energies from 0.1 to 1.0 keV; blue, energies from 1.0 to 7.0 keV; and white, energies greater than 7 keV. These high-energy events are caused by pileup; we emphasize these only to illustrate the unresolved source at the center. Figure courtesy of NASA/SAO/CXC.

relationship to the geometry of the bipolar nebula. The ring for example is not in the equatorial plane as might first be expected. The most likely possibility is that we are seeing clumps of material in an irregular shell, so we will refer to this material as the "outer shell" or simply the "shell," but we will use a partial torus to calculate the density.

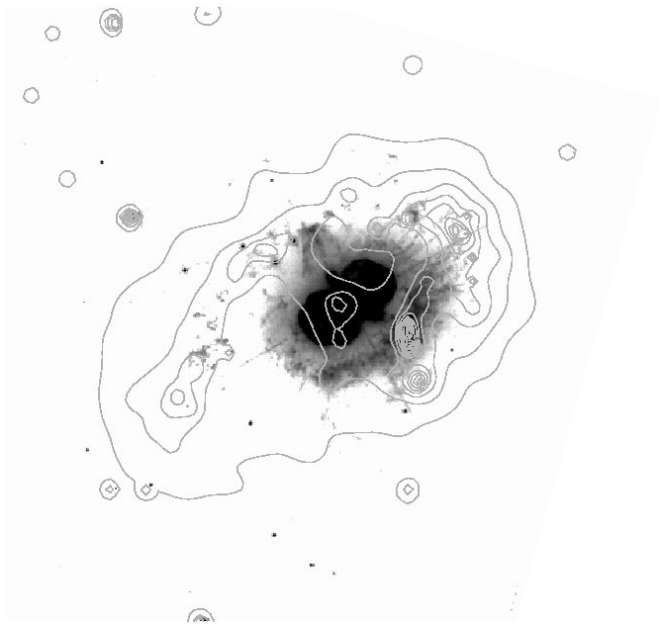

FIG. 2.—Soft X-ray ring overlaid on a λ6590 *HST* image of η Car, printed to show the outer shell. The X-ray ring is clearly associated with the ragged optical knots that form the outer shell. The brightest X-ray knot coincides with the brightest optical knot southwest of the central source. Contour spacing is proportional to the square root of the surface brightness.

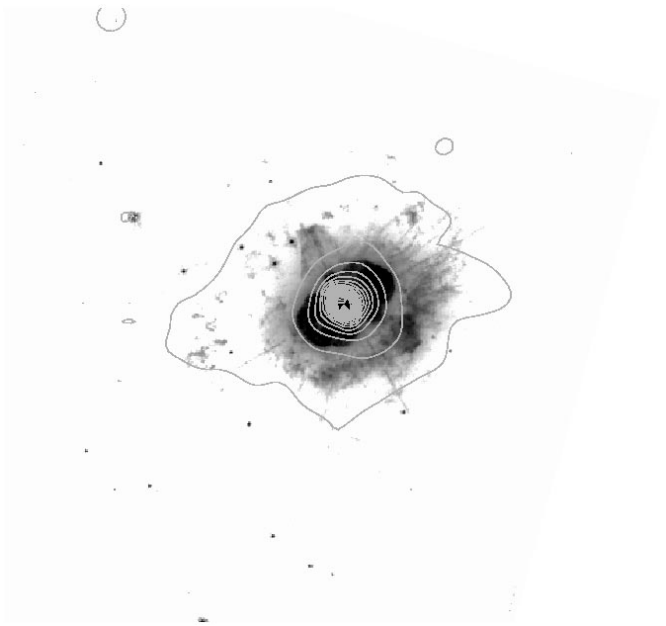

FIG. 3.—Contours of 2.1–8.0 keV surface brightness overlaid on a λ6590 *HST* image of η Car, printed to show the outer shell. Contour spacing is proportional to the square root of the surface brightness. The bright X-ray source is coincident with the central source of the bipolar nebula. Closely spaced contours around this source indicate scattering from the telescope mirror, but the faintest contour partially follows the outer shell.

Figure 1 was made using an adaptive conservative smoothing algorithm (CSMOOTH) to postprocess the η Car images. This smooths a two-dimensional image in such a way that the smoothing scale is increased until the total number of counts under the kernel exceeds a value that is determined from a preset significance and the expected number of background counts in the kernel area. The scale is determined by convolving the raw image with a Gaussian kernel, whose size grows from a small initial value to the maximum allowable value corresponding to the size of the raw image itself.

Data were analyzed using the *Chandra* CIAO software and the FTOOLS XSPEC. Both TE and CC mode data were first cleaned by rejecting ACIS event grades 1, 5, and 7 (*Chandra* X-Ray Center 2000). Since η Car is a bright source, we did not do any background filtering. The ACIS focal-plane temperature at the time of the observation was $-100°$C. Since no calibration has yet been done for this temperature, we used spectral response matrices for $-90°$ and shifted the gain so the model spectrum reproduced the observed Ir (i.e., mirror coating) absorption edge at 2.1 keV. The observed spectral structure indicates that the resolution is close to that observed in the $-90°$ calibrations. The gain shift was also checked against a better-known Cas A spectrum taken a few days earlier. The lack of calibrated response matrices, however, prevents an accurate spectral analysis, particularly at low energies.

3. COMPARISON WITH BIPOLAR NEBULA AND OUTER SHELL

Figure 2 shows 0.1–0.8 keV X-ray emission superimposed on the *HST* WFPC image (courtesy J. Morse 2000) with the F658N filter. This filter is centered at λ6590 and passes N II

λ6583 and scattered Hα (Morse et al. 1998). X-ray emission from the central source is strongly absorbed, so only the extended soft emission from the shell is visible. Note that there are no X-ray features corresponding to the bright optical bipolar nebula. The extended X-ray shell is instead clearly associated with compact knots of line emission, as described by Morse et al. (1998) as being in the "outer debris field," which is the same region as Walborn's "outer shell." The brightest X-ray knot coincides exactly with a bright optical patch in the southwest outer shell (Walborn's "S condensation"). The X-ray maximum, which forms the northwest part of the shell, is at the outer boundary of the debris field (the "W arc"), and the maximum at the southeast extreme of the X-ray shell coincides with the southeast extension of the debris field (the "E condensations").

Figure 3 shows a higher energy band; here 2.1–8.0 keV X-ray brightness contours are superimposed on the same F658N image. The central source now dominates the X-ray image, but there is also a hint of emission from the outer shell. This will be discussed in § 6.

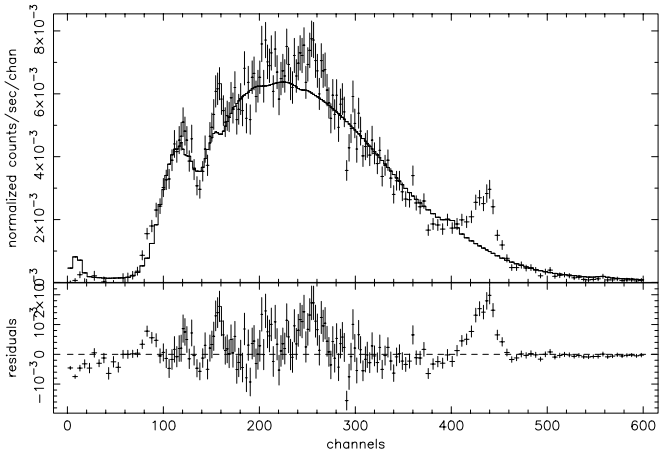

FIG. 4.—X-ray spectrum of the central source taken from the CC mode data. Spectrum is fitted with a bremsstrahlung continuum with $kT = 15$ keV. The notch at channel 140 (2.1 keV) is an absorption edge in the Ir mirror coating. There is a broad Fe emission line at channel 440 (≈6.7 keV) and evidence for emission lines at lower energies. There is no emission below 1.0 keV.

4. THE CENTRAL SOURCE

The central source has a strength of 1.6 counts s^{-1} in the CC mode observation. The TE mode data, with apparent rate 0.17 s^{-1}, is severely distorted by "pileup," a phenomenon in which 2 or more photons register in a single ACIS pixel during its recording interval and are counted as one event having the summed energy of all interacting photons in that pixel. The flux measured at the detector is 4.4×10^{-11} ergs cm^{-2} s^{-1}, and at 2.3 kpc distance, the source luminosity (before absorption in surrounding material and interstellar medium) is $L_X = 6 \times 10^{34}$ ergs s^{-1} in the range 0.2–10 keV. Flux calculations using the PIMMS program (*Chandra* X-Ray Center 2000) are given in Table 1.

Figure 4 shows the pulse-height spectrum of the central source. Since there is no exact calibration, the energy scale is still uncertain. If the Ir edge at 2.1 keV is used for determination, the energy of the prominent Fe line emission is in the range of 6.5–6.8 keV. With this normalization, the general shape of the spectrum is well reproduced using either a power law or a thermal continuum. There are emission lines at energies 2.4 (S), 3.7–4.0 (Ca), and 6.5–6.8 (Fe) keV. If the assumed calibration reproduces the detector response reasonably, there may also be lines at 1.3 (Mg), 1.9 (Si), and 3.2 (A) keV. An absorption of 4×10^{22} atoms cm^{-2} of cold material is required. The continuum fit is not sensitive to temperature in the range $kT = 6$–20 keV. If a Raymond model is used, the Fe emission-line shape seems to require a strong contribution from Fe XXV and/or Fe XXVI at ≈6.8 keV and a kT of ∼15 keV, although both *RXTE* and *ASCA* spectra indicate a temperature of ∼5 keV (Corcoran et al. 2000).

The broad Fe line emission requires at least two components at ∼6.8 and ∼6.5 keV. This is consistent with the report of Corcoran et al. (1998) of an Fe fluorescence line at ∼6.4 keV in the *ASCA* data. A deeper *Chandra* observation is planned with the grating and a well-calibrated ACIS configuration, so we will not elaborate here on the details of these line emissions.

The appearance of the central source in the TE data (Fig. 1) suggests a surrounding halo of scattered X-rays. Figure 5 shows the *Chandra* point-response function (PRF) compared to the radial surface brightness of the central source. The PRF has been weighted according to the measured spectrum and normalized to the counting rate measured in the CC observation. Since pileup is most severe in pixels with the highest counting rate, the central surface brightness is greatly diminished, but there is no distortion apparent at radial distances greater than 2.″5. The surface brightness follows the PRF closely from 2.″5 to 5.″0 radius, so we conclude that there is no observable scattering halo at these radial distances. Even excluding energies below 1.0 keV, some emission remains at larger radial distances. The faint-

TABLE 1

COUNT RATE, FLUX, AND LUMINOSITY

Parameter	Energy Range (keV)	Central Source	Ring
ACIS rate (counts s^{-1})	0.2–10	1.6 ± 0.1	$0.40 \pm .01$
kT (keV)	...	15^{+5}_{-10}	0.3 ± 0.1
N_H (atoms cm^{-2})	...	4×10^{22}	2×10^{21}
Flux: absorbed (ergs cm^{-2} s^{-1})	0.2–10	$4.4^{+0.0}_{-0.7} \times 10^{-11}$	$2.2 \pm 0.3 \times 10^{-12}$
Flux: unabsorbed (ergs cm^{-2} s^{-1})	0.2–10	$8.8 \pm 0.3 \times 10^{-11}$	$1.5^{+1.7}_{-0.5} \times 10^{-11}$
Flux: absorbed (ergs cm^{-2} s^{-1})	2–10	$4.3^{+0.0}_{-0.7} \times 10^{-11}$	...
L_X: no ISM absorption (ergs s^{-1})	0.2–10	$2.8^{+0.0}_{-0.5} \times 10^{34}$	$1.0^{+1.1}_{-0.6} \times 10^{34}$
L_X: no η Car absorption (ergs s^{-1})	0.2–10	$5.6 \pm 0.2 \times 10^{34}$	...

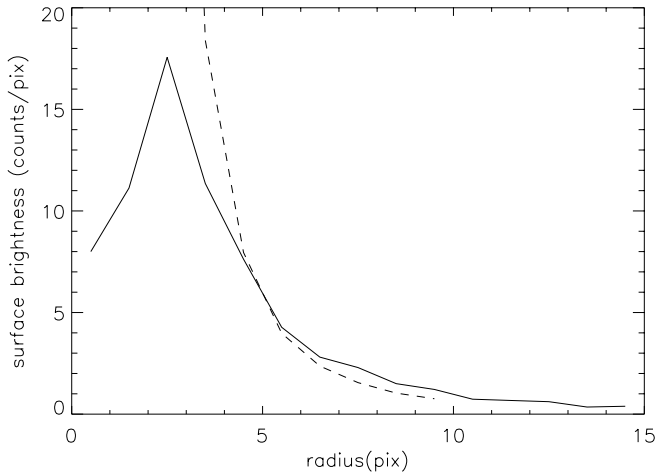

FIG. 5.—The radial surface brightness of the central source compared to a weighted *Chandra* PRF. Solid line is the data, greatly depressed at the center because of pileup. Dashed curve is the PRF, which has an intensity of 10,000 at the source position; 1 ACIS pixel is equal to 0.″5.

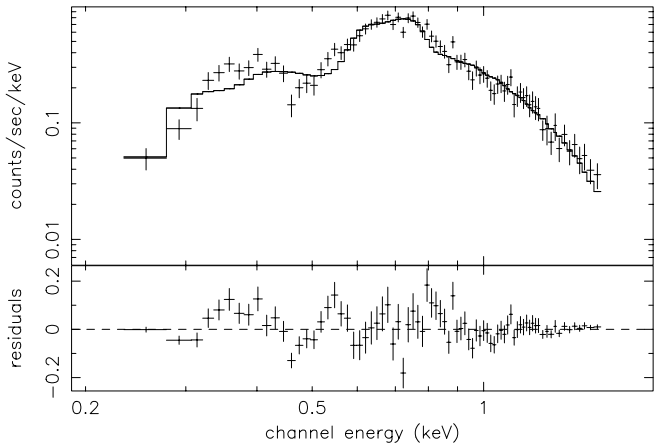

FIG. 6.—X-ray spectrum of the ring. Spectrum is fit with a bremsstrahlung continuum, with $kT = 0.21$ keV and with two emission lines of energies ≈ 0.3 and 0.7 keV.

est contour in Figure 3 follows the morphology of the outer shell indicating some emission from material in this area.

The line of sight to the central source passes through the southeast (nearer) lobe of the bipolar nebula (Morse et al. 1998). The path length inside this lobe is $\approx 10^{17}$ cm, so the observed X-ray–absorbing column of 4×10^{22} atoms cm^{-2} implies a density of $\approx 4 \times 10^5$ atoms cm^{-3} inside the lobe. This is in good agreement with other estimates (Davidson & Humphreys 1997). As the lobe expands and if no more material is injected, the X-ray–absorbing column should decrease with time.

5. THE OUTER SHELL

The emission is soft and at energies above 2 keV the shell almost disappears (note the faint residual seen in Fig. 3). The central source obscures any high-energy diffuse emission which might come from the central region. The geometry is more ringlike than shell-like. The projection of a limb-brightened shell would have more central emission. A shell with a thickness of $\frac{1}{5}$ the radius would have central brightness that is $\approx 40\%$ of the brightest part of the limb. We observe a central brightness only $\approx 15\%$ that of the rim. For the analysis, we assume a ring (torus) with diameter $45'' = 0.50$ pc and thickness (diameter of circular cross section) $7'' = 0.08$ pc. The ring is inclined 45°–50° from the plane of the sky and $\frac{1}{4}$ of the ring is missing. The volume of this partial ring is 1.7×10^{53} cm^3. The brightest knot of emission has projected dimensions $4'' \times 6''$, and assuming an intermediate thickness, the volume is 2.6×10^{51} cm^3.

The spectrum of the shell was obtained by extracting events from an elliptical region including the shell and excluding events from the central source. This spectrum, shown in Figure 6, is a rather smooth continuum with some structure from 0.6 to 0.9 keV. This can be fitted with a bremsstrahlung continuum with kT ranging from 0.2 to 0.4 keV and with lines at ~ 0.4 and ~ 0.7 keV, perhaps from N and Fe L. A Raymond model with cosmic abundances predicts line emission from Ne at ~ 0.9 and from Mg at ~ 1.3, which are not evident in the spectrum. We are not being precise here because the calibration uncertainty increases at low energies. Both effective area and energy scale are not well calibrated, so the existence and identification of spectral features is highly uncertain. Nevertheless, a low-energy feature in *ASCA* spectra was also found by Tsuboi et al. (1997) and by Corcoran et al. (1998), which they identified as attributable to N emission. If this is really an N emission line, the low transmission of the ISM at ~ 0.4 keV implies that the shell is remarkably bright in N emission, an appealing thought since some of the optical knots shine brightly with N line emission (Davidson, Walborn, & Gull 1982; Davidson et al. 1986). The X-ray spectrum of the bright knot is, within the statistics of the ≈ 400 counts collected, the same as that of the whole shell.

The X-ray flux from the shell is 2.2×10^{-12} ergs cm^{-2} s^{-1} measured at the detector, which, using $kT = 0.3$ and $N_{\rm H} = 2 \times 10^{21}$ atoms cm^{-2}, implies an X-ray luminosity of $L_{\rm X} = 1.0 \times 10^{34}$ ergs s^{-1}. Assuming a uniform density throughout the torus, we calculate a density of 50 atoms cm^{-3}. Total thermal energy is 2×10^{46} ergs. Total mass is $1.0 \times 10^{-2}\ M_\odot$. The bright knot contains $4 \times 10^{-4}\ M_\odot$ at a density of 130 atoms cm^{-3}.

Davidson et al. (1986) estimated the amount of UV-emitting material in the S condensation as $\sim .02\ M_\odot$ with electron density $\sim 10^4$ cm^{-3}. The X-ray–emitting gas in the bright knot thus represents only 1% of the material in this region.

Even though the morphology is not convincingly shell-like, could this material be a limb-brightened shell of hot gas behind a blast wave originating in the Great Eruption 160 years ago? The answer is yes. The age of a blast wave can be calculated from the radius and temperature (e.g., Seward & Velusamy 1995); the result is 185^{+105}_{-70} years, which is consistent with the time since the Great Eruption.

An alternate way of heating the X-ray–emitting gas is via the optical knots in the debris field. These have velocities of 300–1300 km s^{-1} (Walborn et al. 1978), implying ejection (with no deceleration) 130–900 years ago. The hot gas in the shell could be preexisting material heated by energy deposited by these fast-moving knots, some of which may have originated in the Great Eruption. Gas temperature and knot velocity are consistent with this process. Indeed, all the knots may have been ejected in 1843 (or even later) with high velocities but have since been decelerated in the outer shell, some more than others. The optical knots show strong line emission, which is thought to be a result of shocks

owing to either high-velocity knots colliding with interstellar clouds or a fast wind impacting cometary knots of material. The X-ray–emitting gas is compatible with either process. Weis, Duschl, & Bomans (2001) show the correlation between kinematics and X-ray emission in great detail.

6. APPLICATION TO MODEL OF THE CENTRAL SOURCE

This *Chandra* observation has satisfactorily confirmed the two-component model used to explain all observations since that of *Einstein*: two components, one soft and one hard, with only the harder radiation coming from the near vicinity of the central object. We now compare the 2–10 keV *Chandra* data with those of *RXTE*, which has been used to define a promising model of the central source. A square degree of sky containing η Car has been monitored since 1997 May with *RXTE* (Corcoran et al. 2001). The 2–10 keV flux observed varies, usually smoothly, from 5×10^{-11} to 16×10^{-11} ergs cm^{-2} s^{-1}, with some fluctuations at high intensity. There is also a 3 month minimum, interpreted as an eclipse, during which the flux drops, not to zero, but to a minimum of 0.5×10^{-11} ergs cm^{-2} s^{-1}. *ASCA* spectra obtained from a 3′ diameter region during this time yield a flux of 5.7×10^{-11} ergs cm^{-2} s^{-1} (2–10 keV) in the "high" state and 0.43×10^{-11} ergs cm^{-2} s^{-1} in the low "eclipsed" state (Corcoran et al. 2000). If this 2–10 keV emission observed during the eclipse is from η Car itself, it has a significant impact on the model.

The currently proposed model ascribes the 2–10 keV X-ray flux to shocked emission from a wind-wind collision in a massive binary system. In this binary model (Corcoran et al. 2001), at the time of the *Chandra* observation the wind-wind collision shock is about 15 AU $\approx 7 \times 10^{-3}$ arcsec from the more massive star and so would be unresolved to *Chandra*. As noted by Corcoran et al. (2000), the *ASCA* X-ray spectrum of η Car during the X-ray low state in 1997 December is *inconsistent* with the colliding-wind binary model, since the colliding wind source should be completely hidden during the eclipse (which is caused by absorption in the wind from the primary star). Perhaps, the 2–10 keV emission seen by *ASCA* at that time is produced by another source of hard emission in the *ASCA* extraction region (a circle of 3′ radius around η Car). We can search for this in the *Chandra* data.

The 2–10 keV flux measured by *Chandra* in CC mode (Fig. 4) is 4.4×10^{-11} ergs cm^{-2} s^{-1} and is almost all from the vicinity of the central source. A near-simultaneous observation with *RXTE* (Corcoran et al. 2000) measures 6×10^{-11} ergs cm^{-2} s^{-1}. This discrepancy probably illustrates the uncertainty in absolute flux measured by different instruments. No other significant sources of 2–10 keV emission are seen in the field. There are, however, at least 50 weak serendipitous sources (almost all are stars in the cluster Trumpler 16) within 5′ of η Car. There is also weak diffuse emission above 2 keV observed from the outer shell, which is well within the region covered by *ASCA*.

In the range 2–10 keV, we observe a small bright halo around the central source that is attributable to the telescope PRF. Assuming that the flux from η Car does not vary between the CC and TE mode observations, the 2–10 keV diffuse flux at radial distances greater than 10″ is in excess of that expected in the "wing" of the telescope PRF.

In an annulus defined by radii 10″ and 90″ in the 2–10 keV band, the observed count rate is 5.5% that of the central source. The *Chandra* mirror PRF indicates that mirror scattering should be $\approx$3.5%. The nine brightest serendipitous sources account for 0.2%, so there is a residual diffuse emission intrinsic to the region with a strength $\approx$2% that of the central source or about 8×10^{-13} ergs cm^{-2} s^{-1}. The residual measured by *ASCA* during eclipse minimum was $\approx$5% of the maximum source strength. We conclude that, although half of the *ASCA*-measured eclipse residual might be diffuse, the other half must come from a region very close to η Car within a *Chandra* resolution element of $\sim$0.″5 or within $\sim$1000 AU of the central star. Speckle interferometry from the ground (Weigelt & Ebersberger 1986) and direct imaging from space (Morse et al. 1998) have revealed the presence of starlike knots, the Weigelt blobs, within 0.″4 of η Car; it is possible that scattering of the colliding wind emission by one or more of these knots produces the 2–10 keV emission seen in the *ASCA* low-state spectrum and may be also responsible for the Fe fluorescent line detected in the *ASCA* spectra. It is also possible that the X-ray–emitting region is not completely eclipsed and the model needs to account for this.

We thank Roberta Humphreys for helpful suggestions and for pointing out several vital references, thus saving us the embarrassment of seeming to ignore work which defines the nature of this peculiar object. Financial support was provided by the *Chandra* X-ray Center NASA contract NAS8-39073.

REFERENCES

Chlebowski, T., Seward, F. D., Swank, J., & Szymkowiak, A. 1984, ApJ, 281, 665
Corcoran, M. F., et al. 1998, ApJ, 494, 381
Corcoran, M. F., Fredericks, A. C., Petre, R., Swank, J. H., & Drake, S. A. 2000, ApJ, 545, 420
Corcoran, M. F., Ishibashi, K., Swank, J. H., & Petre, R. 2001, ApJ, 547, 1034
Corcoran, M. F., Rawley, G. L., Swank, J. H., & Petre, R. 1995, ApJ, 445, L121
Chandra X-Ray Center. 2000, in *Chandra* Proposers' Observatory Guide, TD 403.00.003, Chandra Project Science & IPI Teams
Davidson, K., Dufour, R. J., Walborn, N. R., & Gull, T. R. 1986, ApJ, 305, 867
Davidson, K., & Humphreys, R. M. 1997, ARA&A, 35, 1
Davidson, K., Walborn, N. R., & Gull, T. R. 1982, ApJ, 254, L47
Davidson, K., et al. 1999, AJ, 118, 1777
Hester, J. J., et al. 1991, AJ, 102, 654
Humphreys, R. M., & Davidson, K. 1994, PASP, 106, 1025
Humphreys, R. M., Davidson, K., & Smith, N. 1999, PASP, 111, 1124
Ishibashi, K., Corcoran, M. F., Davidson, K., Swank, J. H., Petre, R., Drake, S. A., Damineli, A., & White, W. 1999, ApJ, 524, 983
Morse, J., Davidson, K., Bally, J., Ebbets, D., Balick, B., & Frank, A. 1998, AJ, 116, 2443
Seward, F. D., & Velusamy, T. 1995, ApJ, 439, 715
Smith, N., & Gehrz, R. D. 1998, AJ, 116, 823
Smith, N., Gehrz, R. D., & Krautter, J. 1998, AJ, 116, 1332
Tsuboi, Y., Koyama, K., Sakano, M., & Petre, R. 1997, PASJ, 49, 85
Walborn, N. M. 1976, ApJ, 204, L17
Walborn, N. M., Blanco, B. M., & Thackeray, A. D. 1978, ApJ, 219, 498
Weigelt, G., & Ebersberger, J. 1986, A&A, 163, L5
Weis, K., Duschl, W. J., & Bomans, D. J. 2001, A&A, 367, 566
Weisskopf, M. C., O'Dell, S. L., & Van Speybroeck, L. P. 1996, Proc. SPIE, 2805, 2
Westphal, J. A., & Neubebauer, G. 1969, ApJ, 156, L45